

# Preparation and electrocatalytic activity of Pt/Ti nanostructured electrodes

Long-Biao Lai, Dong-Hwang Chen\* and Ting-Chia Huang

Department of Chemical Engineering, National Cheng Kung University, Tainan, Taiwan, 701, R.O.C. E-mail: chendh@mail.ncku.edu.tw; Fax: 886-6-2344496; Tel: 886-6-2757575 Ext. 62680

Received 12th October 2000, Accepted 26th February 2001  
First published as an Advance Article on the web 3rd April 2001

Pt/Ti nanostructured electrodes have been prepared first by the electrophoretic deposition of Pt nanoparticles (7.4 and 11.1 nm) on a Ti support in reverse micellar solutions of water/Aerosol OT/isooctane, followed by heat treatment in air at 400–600 °C. The crystal structures of the resultant electrodes were characterized by XRD, and their electrocatalytic activities were investigated by cyclic voltammetry in a mixed solution of 0.26 M HCOOH and 1.0 M HClO<sub>4</sub>. The effects of the heat-treatment temperature and the size of the Pt nanoparticles were examined. It was observed that the electrocatalytic activity of the resultant Pt/Ti electrode for the oxidation of HCOOH was much higher than that of a bulk Pt electrode. With increases in the heat-treatment temperature and size of the Pt nanoparticles, the electrocatalytic activity of the Pt/Ti electrode decreased due to sintering and the reduction of the specific surface area. According to the cyclic voltammetric and XRD analyses, it was suggested that the resultant Pt/Ti electrode had lower percentages of Pt(100) and Pt(111) planes but a higher percentage of Pt(110) planes than the bulk Pt electrode. As the heat-treatment temperature increased, both the percentages of Pt(100) and Pt(111) planes increased but the percentage of Pt(110) planes decreased.

## Introduction

It is known that Pt is the most active catalyst for hydrogen evolution and oxidation reactions. However, the commercial use of Pt as a cathode for water electrolysis is very limited because of the high cost. In addition to the utilization of cheaper materials such as Ni and Ni-based alloys, one way to overcome this problem is to develop an electrode containing less Pt but with a larger surface area for catalytic reactions. Recently, nanostructured materials have attracted increasing attention because they exhibit unusual electronic, optical, magnetic, and chemical properties significantly different from those of conventional bulk materials due to their extremely small size or large specific surface area.<sup>1–3</sup> Based on the reduction in the Pt amount required and the possible presence of special electrochemical properties, the development of Pt nanostructured electrodes hence becomes an important and interesting topic.

Until now only a few reports on the preparation and characterization of Pt nanostructured electrodes have been proposed. They were focused primarily on glassy carbon-supported Pt (Pt/GC) nanostructured electrodes prepared by vacuum evaporation,<sup>4</sup> pulsed electrodeposition,<sup>5</sup> and electroplating.<sup>6</sup> Recently, the utilization of electrophoretic deposition for the preparation of nanostructured thin films has received the attention of Giersig and Mulvaney,<sup>7</sup> Trau *et al.*,<sup>8–10</sup> Solomentsev *et al.*,<sup>11</sup> and Teranishi *et al.*<sup>12</sup> However, their studies emphasized the preparation of ordered nanoparticle monolayers on copper grids, or the investigation of hydrodynamic models by observing the assembly of micrometer-size polystyrene latex particles on the electrode. Larger scale multilayered thin films fabricated directly from nanoparticle dispersions have been seldom prepared by electrophoretic deposition,<sup>13</sup> although this process has been used extensively to fabricate bulk products and films from suspensions of micrometer-sized ceramic particles.<sup>14</sup> In this study, a Pt nanostructured electrode was prepared by the electrophoretic

deposition of Pt nanoparticles on a Ti support followed by a heat treatment. Since the oxidation of formic acid has been studied extensively in recent decades due to its potential applications in practical fuel cells and the process of methanol oxidation,<sup>15–17</sup> the electrocatalytic activity of the resultant Pt/Ti electrode was described by investigating the electrocatalytic oxidation of formic acid.

## Experimental

Hydrogen hexachloroplatinate(IV) hydrate was obtained from Acros Organics (Belgium). Hydrazinium hydroxide, formic acid, and perchloric acid were guaranteed reagents from E. Merck (Darmstadt). Reagent-grade acetone and hydrochloric acid were supplied by Kanto Chemical Co. (Tokyo). Sodium di-2-ethylhexylsulfosuccinate (Aerosol OT) purchased from Sigma Chemical Co. (St. Louis, MO) was vacuum dried at 60 °C for 24 h and stored in a vacuum desiccator prior to use. HPLC-grade isooctane supplied by TEDIA (Fairfield) was dehydrated with molecular sieves 4 Å (8–12 mesh, Janssen) for at least 24 h and kept in a vacuum desiccator before use. The residual water of the isooctane solution of Aerosol OT was found to be negligible using a Karl-Fisher moisture titrator (Kyoto Electronics MKC-500). The water used throughout this work was reagent-grade water produced by using a Milli-Q SP Ultra-Pure-Water Purification System of Nihon Millipore Ltd., Tokyo. Before use, Ti supports were first degreased with soap and water, then etched for 1 h in a 6 M HCl solution at 80–90 °C, ultrasonically cleaned with water and acetone, and finally dried in air.

The Pt nanoparticles were prepared in reverse micelles of water/Aerosol OT/isooctane at 25 °C according to our previous work.<sup>18</sup> The reverse micellar solutions containing H<sub>2</sub>PtCl<sub>6</sub> or hydrazine were prepared by injecting the required amounts of the corresponding aqueous solutions into an isooctane solution of Aerosol OT. The monodispersed Pt nanoparticles were

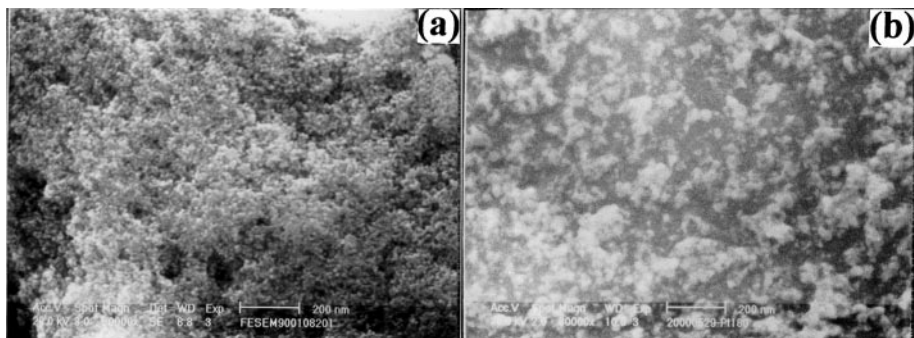


Fig. 1 SEM micrographs for the Ti-supported Pt nanostructured electrodes treated at 400 °C (a) and 600 °C (b).

obtained by mixing equal volumes of two reverse micellar solutions at the same molar ratio of water to Aerosol OT ( $\omega_o$ ) and Aerosol OT concentration (0.1 M), one containing an aqueous solution of  $H_2PtCl_6$  (0.1 M) and the other containing an aqueous solution of hydrazine (1.0 M). The concentration of Aerosol OT was based on the overall volume of the reverse micellar solution, while the concentrations of  $H_2PtCl_6$  and hydrazine were referred to the volume of aqueous solution added into the reverse micellar solution. The mean diameters of Pt nanoparticles obtained at  $\omega_o=5$  and 10 were 7.4 and 11.1 nm, respectively.<sup>18</sup>

The electrophoretic deposition was carried out at 25 °C with an 18 mL reverse micellar solution containing 1.64 mg Pt nanoparticles in a glass cell. The Ti support and Pt sheet were used as the cathode and anode, respectively. The spacing between the electrodes was 0.5 cm, and the geometric surface area of the Ti support for the deposition of Pt nanoparticles was 0.56 cm<sup>2</sup>. During the electrophoretic deposition of Pt nanoparticles, the solution gradually turned from dark brown to clear. It was found that the time required for the complete deposition of Pt nanoparticles onto the Ti support decreased with increasing the electric field strength or decreasing the concentration of Pt nanoparticles. When the electric field strength was below 600 V cm<sup>-1</sup>, the deposition of Pt nanoparticles onto the Ti support was quite insignificant, even after 8 h. However, when the electric field strength was above 1200 V cm<sup>-1</sup>, the coagulation of Pt nanoparticles occurred in the solution. Therefore, an appropriate electric field strength of 1000 V cm<sup>-1</sup> was used throughout this work. Under this condition, the time required for the complete deposition of Pt nanoparticles onto the Ti support was about 3 h. After deposition, the as-prepared Pt/Ti electrode was removed from the solution and heated in air at the required heat-treatment temperature for 5 min to achieve the sintering of Pt nanoparticles and strengthen their bonding to the Ti support, since the Pt nanoparticles for the unheated sample and those heated below 200 °C peeled off the Ti support slightly. The appropriate heat-treatment temperature was 400–600 °C. In this temperature range, this method for the fabrication of electrodes is reproducible. After heat-treatment, the electrode finally was annealed in air for more than 3 h. In this work, unless otherwise stated, the mean diameter of Pt nanoparticles used for the preparation of Pt/Ti nanostructured electrodes was 7.4 nm and the heat-treatment temperature was 400 °C.

The cyclic voltammetric measurement of Pt/Ti nanostructured electrodes was conducted in a mixed solution of 0.26 M HCOOH and 1.0 M HClO<sub>4</sub> at 25 °C using the Electrochemical Analyzer System, BAS CV-50W (Bioanalytic System, Inc.). The steady-state cyclic voltammograms were obtained after about twenty cycles. An Ag/AgCl electrode and a Pt wire were used as the reference and counter electrodes, respectively. The tip of the reference electrode was set at a distance of 0.5 cm from the surface of the working electrode to minimize the error caused by the *iR* drop in the solution. Before measurement, the solution was degassed with purified nitrogen gas for 15 min,

and the working electrodes were polarized from 0 to 1.5 V at 100 mV s<sup>-1</sup> for 10 min in 1.0 M HClO<sub>4</sub> solution. The sweep rate was fixed at 50 mV s<sup>-1</sup>. All potentials were given on the reversible hydrogen electrode (RHE) scale, and the current densities were the values based on the geometric surface area of the electrode. A Pt sheet (99.9% pure) with a geometric surface area of 0.56 cm<sup>2</sup> was used as the bulk Pt electrode.

## Results and discussion

Fig. 1 shows typical SEM micrographs for Ti-supported Pt nanostructured electrodes derived from Pt nanoparticles of 7.4 nm treated at 400 and 600 °C, showing that Pt nanoparticles can be electrophoretically deposited onto a Ti support. For the electrode treated at 400 °C, the Pt nanoparticles deposited on the Ti support could be obviously seen. This revealed directly the formation of the Pt/Ti nanostructured electrode. When the heat-treatment temperature was raised to 600 °C, the sintering of Pt nanoparticles was significant. Thus, a higher heat-treatment temperature than 600 °C should be unnecessary.

The XRD patterns of the Ti-supported Pt nanostructured electrodes treated at 400 and 600 °C are shown in Fig. 2. The characteristic peaks located at  $2\theta=40, 46,$  and  $67^\circ$  represent the (111), (200), and (220) lattice planes of Pt, respectively. This revealed that the particles on the Ti support were pure Pt of face-centered cubic (fcc) structure. Furthermore, the ratios of the intensity of the Pt(200) plane to that of the sum of Pt(111) and Pt(220) planes for the Pt/Ti electrodes treated at 400 °C and 600 °C were 0.250 and 0.283, respectively. This implied that the amount of Pt(100) plane parallel to the Pt(200) plane increased with increasing heat-treatment temperature.

Fig. 3 shows the steady-state cyclic voltammograms of typical Pt/Ti and bulk Pt electrodes in a mixed solution of 0.26 M HCOOH and 1.0 M HClO<sub>4</sub>. The features are essentially similar. In Fig. 3(a), two anodic peaks appear in the positive-going scan: P<sub>1</sub> at 0.6 V and P<sub>2</sub> at 0.94 V. In the negative-going

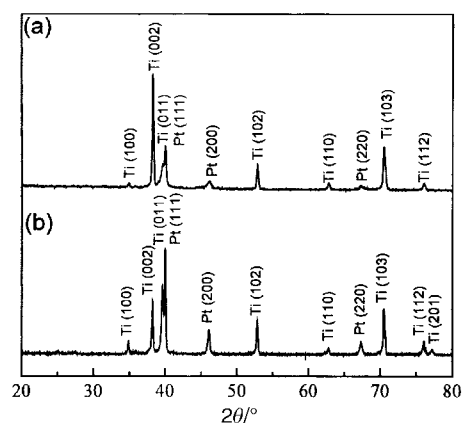
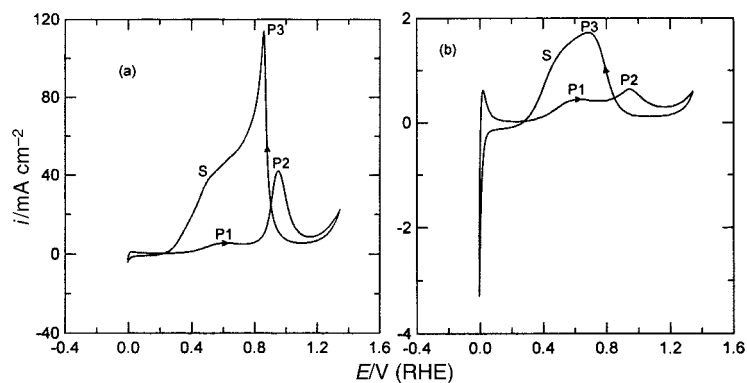
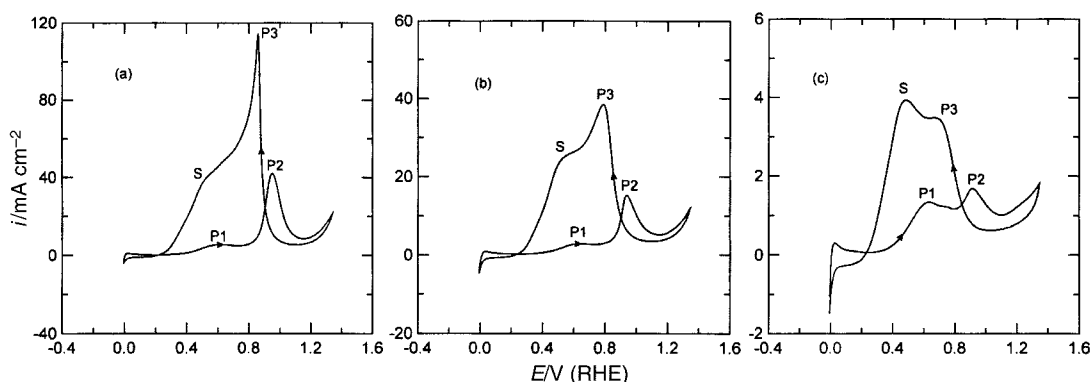


Fig. 2 XRD patterns of the Pt/Ti nanostructured electrodes treated at 400 °C (a) and 600 °C (b).



**Fig. 3** Steady-state cyclic voltammograms of a typical Pt/Ti electrode treated at 400 °C (a) and a bulk Pt electrode (b) in a mixed solution of 0.26 M HCOOH and 1.0 M HClO<sub>4</sub>.



**Fig. 4** Steady-state cyclic voltammograms of Pt/Ti electrodes treated at 400 °C (a), 500 °C (b), and 600 °C (c) in a mixed solution of 0.26 M HCOOH and 1.0 M HClO<sub>4</sub>.

scan, another anodic peak P<sub>3</sub> at 0.85 V and a shoulder peak S at 0.5 V appear. All these characteristic peaks are similar to those usually observed for polycrystalline Pt electrodes<sup>19–26</sup> and can be described as follows. In the positive-going scan, formic acid adsorbs and dissociates on Pt surfaces *via* the hydrogen atoms, and the formed CO retards the reaction strongly up to 0.8 V.<sup>19–21</sup> The peak P<sub>1</sub> can be attributed to the oxidation of formic acid (HCOOH → active intermediate → CO<sub>2</sub><sup>15</sup>) on Pt(111) planes.<sup>22–26</sup> The peak P<sub>2</sub> is due to the oxidation of the adsorbed CO.<sup>27,28</sup> In the negative-going scan, the peaks P<sub>3</sub> and S can be attributed to the oxidation of formic acid through the active intermediate on Pt(110) and Pt(100) planes, respectively.<sup>26</sup> The larger peaks, compared with peaks P<sub>1</sub> and P<sub>2</sub>, are due to the fact that the adsorbed CO has been oxidized to be CO<sub>2</sub> at peak P<sub>2</sub>. Comparing Fig. 3(a) and 3(b), it is obvious that the current density of the Pt/Ti electrode was much higher than that of the bulk Pt electrode. The total charge passed through peaks P<sub>1</sub>, P<sub>3</sub>, and S for the Pt/Ti electrode and that for the bulk Pt electrode were evaluated to be 342 and 9.16 mC, respectively. This revealed that the electrocatalytic activity of the Pt/Ti electrode was much higher (37 times) than that of the bulk Pt electrode. That is, the resultant Pt/Ti electrode had a significantly larger specific surface area than the bulk Pt electrode.

According to Fig. 3(a), the current densities of P<sub>1</sub>, P<sub>3</sub>, and S for the Pt/Ti electrode were 6.15, 113.8, and 38.2 mA cm<sup>-2</sup>, respectively. Based on the current density of P<sub>1</sub>, their relative ratios were 1 : 18.5 : 6.2. For the bulk Pt electrode, as indicated in Fig. 3(b), the current densities of P<sub>1</sub>, P<sub>3</sub>, and S were 0.424, 1.703, and 1.329 mA cm<sup>-2</sup>, respectively, and their relative ratios were 1 : 4.0 : 3.1. This suggested that the resultant Pt/Ti electrode has lower percentages of Pt(100) and Pt(111) planes but a higher percentage of Pt(110) planes than the bulk Pt electrode.

Fig. 4 shows the steady-state cyclic voltammograms for the Pt/Ti electrodes treated at 400, 500, and 600 °C. It was observed that the current density decreased with increasing heat-treatment temperature. The total charges passed through peaks P<sub>1</sub>, P<sub>3</sub>, and S during the oxidation of HCOOH for the Pt/Ti electrodes treated at 400, 500, and 600 °C were 342, 171, and 25 mC, respectively. The decrease in the current density or total charge with the increase of temperature could be attributed to the reduction of specific surface area caused by sintering. Moreover, the current densities of P<sub>1</sub>, P<sub>3</sub>, and S for the Pt/Ti electrode treated at 500 °C were 2.85, 38.2, and 24.1 mA cm<sup>-2</sup>, respectively. Their relative ratios were 1 : 13.4 : 8.5. The current densities of P<sub>1</sub>, P<sub>3</sub>, and S for the Pt/Ti electrode treated at 600 °C were 1.32, 3.41, and 3.91 mA cm<sup>-2</sup>, respectively. Their relative ratios were 1 : 2.58 : 2.96. Thus, according to the relative ratios for the bulk Pt and the Pt/Ti electrodes treated at 400–600 °C, it could be observed that both the percentages of Pt(100) and Pt(111) planes increased but the percentage of Pt(110) planes decreased with increasing heat-treatment temperature. This result is consistent with the XRD analysis and might result from the sintering during heat treatment. In addition, it was also noted that the percentages of Pt(100) and Pt(111) planes for the Pt/Ti electrode treated at 600 °C were larger than those for the bulk electrode. This may result from their different preparation processes.

The steady-state cyclic voltammograms for the Pt/Ti electrodes derived from Pt nanoparticles of 7.4 and 11.1 nm are shown in Fig. 5. It is observed that the current density decreased with increasing size of the Pt nanoparticles. The total charge passed through peaks P<sub>1</sub>, P<sub>3</sub>, and S during the oxidation of HCOOH for the Pt/Ti electrode derived from Pt nanoparticles of 11.1 nm was 176 mC, lower than that derived from the Pt nanoparticles of 7.4 nm (342 mC). Since the amounts of Pt

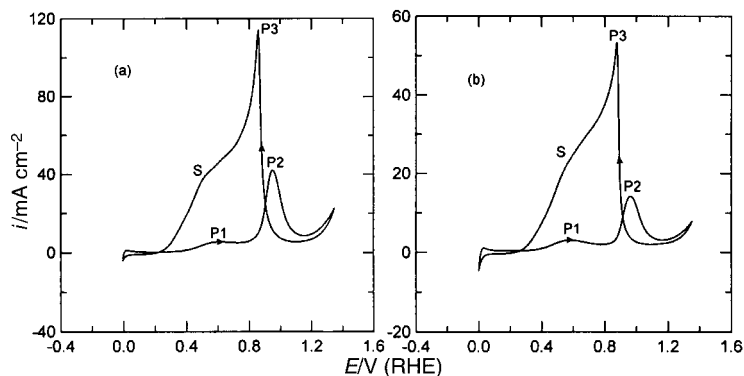


**Fig. 5** Steady-state cyclic voltammograms of Pt/Ti electrodes treated at 400 °C in a mixed solution of 0.26 M HCOOH and 1.0 M HClO<sub>4</sub>. Mean diameter of Pt nanoparticles: 7.4 nm (a) and 11.1 nm (b).

deposited on the Ti supports were the same, this result indicates that the Pt/Ti electrode derived from Pt nanoparticles of 7.4 nm had a larger specific surface area than that derived from Pt nanoparticles of 11.1 nm. This is consistent with the expectation that electrodes with larger specific surface areas may be obtained by the use of smaller particles.

Other nanostructured Pt electrodes, prepared by vacuum evaporation, pulsed electroposition and electroplating,<sup>5,29,30</sup> usually have high specific surface areas. However, only a low loading of Pt on the electrode is possible for them. Therefore, their current densities are much lower than ours.<sup>4</sup> Consequently, the nanostructured Pt electrodes developed in this work may be more useful in practical applications.

## Conclusions

Pt/Ti nanostructured electrodes have been successfully prepared first by the electrophoretic deposition of Pt nanoparticles followed by heat treatment on a Ti support. Comparing with the bulk Pt electrode, the obtained Pt/Ti electrode exhibited significantly higher electrocatalytic activity for the oxidation of HCOOH and had lower percentages of Pt(100) and Pt(111) planes but a higher percentage of Pt(110) planes. As the heat-treatment temperature increased, the electrocatalytic activity of the Pt/Ti electrode decreased, and both the percentages of Pt(100) and Pt(111) planes increased but the percentage of Pt(110) planes decreased. It was also found that the electrocatalytic activity of the Pt/Ti electrode could be raised by the use of smaller Pt nanoparticles. This work should be helpful for the development of nanostructured electrodes and the commercial use of Pt as a cathodic material for water electrolysis.

## Acknowledgements

This work was performed under the auspices of the National Science Council of the Republic of China, under contract number NSC 87-2214-E006-010, to which the authors wish to express their thanks.

## References

- 1 C. Hayashi, *Phys. Today*, 1987, **40**, 44.
- 2 H. Gleiter, *Prog. Mater. Sci.*, 1989, **33**, 223.
- 3 R. Uyeda, *Prog. Mater. Sci.*, 1991, **35**, 1.
- 4 K. Yahikozawa, Y. Fujii, Y. Matsuda, K. Nishimura and Y. Takasu, *Electrochim. Acta*, 1991, **36**, 973.
- 5 J. L. Zubimendi, G. Andreassen and W. E. Triaca, *Electrochim. Acta*, 1995, **40**, 1305.
- 6 W. Vogel, L. Lundquist, P. N. Ross and P. Stonehart, *Electrochim. Acta*, 1975, **20**, 79.
- 7 M. Giersig and P. Mulvaney, *Langmuir*, 1993, **9**, 3408.
- 8 M. Trau, S. Sankaran, D. A. Saville and I. A. Aksay, *Nature*, 1995, **374**, 437.
- 9 M. Trau, D. A. Saville and I. A. Aksay, *Science*, 1996, **272**, 706.
- 10 M. Trau, D. A. Saville and I. A. Aksay, *Langmuir*, 1997, **13**, 6375.
- 11 Y. Solomentsev, M. Böhmer and J. L. Anderson, *Langmuir*, 1997, **13**, 6058.
- 12 T. Teranishi, M. Hosoe and M. Miyake, *Adv. Mater.*, 1997, **9**, 65.
- 13 E. M. Wong and P. C. Searson, *Chem. Mater.*, 1999, **11**, 1959.
- 14 P. Sarkar and P. S. Nicholson, *J. Am. Ceram. Soc.*, 1996, **79**, 1987.
- 15 R. Parsons and T. Vandernoot, *J. Electroanal. Chem.*, 1988, **257**, 9.
- 16 A. Capon and R. Parsons, *J. Electroanal. Chem.*, 1973, **44**, 1.
- 17 M. R. Columbia and P. A. Thiel, *J. Electroanal. Chem.*, 1994, **369**, 1.
- 18 D. H. Chen, J. J. Yeh and T. C. Huang, *J. Colloid Interface Sci.*, 1999, **215**, 159.
- 19 H. Kita and H. W. Lei, *J. Electroanal. Chem.*, 1995, **388**, 167.
- 20 K. Kunitatsu, *J. Electroanal. Chem.*, 1986, **213**, 149.
- 21 J. Clavilier and S. G. Sun, *J. Electroanal. Chem.*, 1987, **236**, 95.
- 22 S. Motoo and N. Furuya, *J. Electroanal. Chem.*, 1985, **184**, 303.
- 23 J. Clavilier and S. G. Sun, *J. Electroanal. Chem.*, 1986, **199**, 471.
- 24 S. C. Chang, L. W. H. Leung and M. J. Weaver, *J. Phys. Chem.*, 1990, **94**, 6013.
- 25 R. R. Adžić, A. V. Tripković and W. E. O'Grady, *Nature*, 1982, **296**, 137.
- 26 T. Iwasita, X. Xia, E. Herrero and H. D. Liess, *Langmuir*, 1996, **12**, 4260.
- 27 E. Herrero, J. M. Feliu and A. Aldaz, *J. Electroanal. Chem.*, 1994, **368**, 101.
- 28 E. Herrero, A. Fernandez-Vega, J. M. Feliu and A. Aldaz, *J. Electroanal. Chem.*, 1993, **350**, 73.
- 29 Y. Takasu, Y. Fujii, K. Yasuda, Y. Iwanaga and Y. Matsua, *Electrochim. Acta*, 1989, **34**, 453.
- 30 P. Stonehart and J. Lundquist, *Electrochim. Acta*, 1973, **18**, 907.